Analyst

Accepted Manuscript

ROYAL SOCIETY OF CHEMISTRY

www.rsc.org/analyst

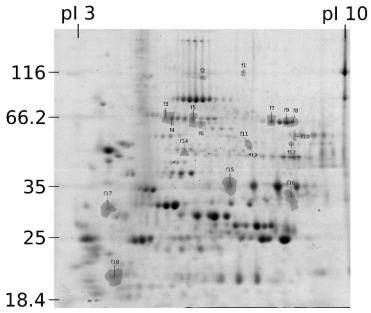

Using a redox-proteomics approach, this study demonstrates that silver nanoparticles and $AgNO_3$ affect the proteome differently, indicating different biological impacts.

ARTICLE TYPE
www. rsc.org/xxxxxx | XXXXXXXX

Proteomic evaluation of citrate-coated silver nanoparticles toxicity in *Daphnia magna*

Louis-Charles Rainville,*[a] Darragh Carolan,[b] Ana Coelho Varela,[c] Hugh Doyle,[b] and David Sheehan[a]

Received Xth XXXXXXXXXX 20XX, Accepted Xth XXXXXXXXX 20XX
First published on the web Xth XXXXXXXXXX 200X
DOI: 10.1039/b000000x

Recent decades have seen a strong increase in the promise and uses of nanotechnology. This is correlated with their growing release in the environment and there is concern that nanomaterials may endanger ecosystems. Silver nanoparticles (AgNPs) have some of the most varied applications, making their release into the environment unavoidable. In order to assess their potential toxicity in aquatic environments, the acute toxicity of citrate-coated AgNPs to *Daphnia magna* was measured and compared to that of $AgNO_3$. AgNPs were found to be ten times less toxic by mass than silver ions, and most of this toxicity was removed by ultracentrifuging. At the protein level, the two forms of silver had different impacts. Both increased protein thiol content, while only AgNP increased carbonyl levels. In 2DE of samples labelled for carbonyls, no feature was significantly affected by both compounds, indicating different modes of toxicity. Identified proteins showed functional overlap between the two compounds: vitellogenins (vtg) were present in most features identified, indicating their role as a general stress sensor. In addition to vtg, hemoglobin levels were increased by the AgNP exposure while 14-3-3 protein (a regulatory protein) carbonylation levels were reduced by $AgNO_3$. Overall, this study confirms the previously observed lower acute toxicity of AgNPs, while demonstrating that the toxicity of both forms of silver follow somewhat different biologic pathways, potentially leading to different interactions with natural compounds or pollutants in the aquatic environment.

1 Introduction

The last decade has seen a sharp increase in the number of studies concerned with the environmental impact of engineered nanoparticles (NP). This concern is fueled by the increasing variety of uses for NP, and their continued development. This is leading to increased NP usage and release in the environment[1].

The novel properties of materials at the nanoscale makes evaluation of their toxicity particularly challenging. Size, surface chemistry, coating, method of suspension and composition all affect the laboratory-based measurement of their toxicity. Although generation of reactive oxygen species (ROS) is a frequent component of NP toxicity[2], the impressive range of NP being manufactured currently means that no general rule can be used to infer their toxicity.

Silver NP (AgNP) are the most widely used commercial nanoparticles, with applications in textiles, medical equipment and household products, mostly involving their antibacterial properties[3]. Their widespread use leads to their release into the environment through their leakage and disposal[4]. Additionally, their behaviour in the environment and in wastewater treatment plants is still a subject of study[4,5]. There is thus a need to understand their interaction with biota, especially in the aquatic environment, where the particles will most likely end up.

As many studies highlight their potential toxicity[6–8], efforts to discern their mechanism of action are becoming more frequent. Yet, the prior knowledge required to properly deploy traditional, hypothesis-based, biomarkers to study AgNP toxicity is still lacking. There is thus an interest in exploiting omics-based tools to gain a better understanding of their toxicity mechanism and to discriminate it from that of their bulk components. This strategy was used by Poynton *et al.* [8] as they applied transcriptomics to identify changes in gene expression following exposure to citrate-coated AgNP, PVP-coated AgNP as well as silver nitrate. This led them to conclude that toxicity of AgNP differed from that of silver nitrate at the mechanistic level and, to a lesser extent, varied with different NP coatings.

In addition to knowledge gained from gene expression studies, the study of proteins is of particular interest in toxicology as they are the principal quantitative targets of toxicity and their covalent modification can lead to various changes

[a] *Proteomics Research Group, School of Biochemistry and Cell Biology, University College Cork, Western Gateway Building 3.99, Western Road, Cork, Ireland. E-mail: louischarles.rainville@gmail.com*
[b] *Tyndall National Institute, University College Cork, Lee Maltings, Cork, Ireland.*
[c] *Instituto de Technologica Quimica e Biologica, Universidade Nova de Lisboa, Av. da República, 2780-157 Oeiras, Portugal.*

in metabolism and cell signaling[9]. Additionaly, proteins are the first targets of the reactive oxygen species (ROS) that accumulate in cells experiencing oxidative stress (OS). Many of their residues can be directly oxidised by ROS, thus serving as buffers, protecting DNA in cells and avoiding irreparable damage. Redox-proteomics are used to study redox-based changes within the proteome[10] enabling a direct detection of lesions caused by the toxicant and of responses at the protein level.

Cysteine, tyrosine and methionine are particularly sensitive to oxidation and their modifications are often measured in redox-proteomics[11]. Protein carbonyls are the most prevalent oxidative lesion of proteins[12] and there is growing evidence of their involvment in signal transduction[13]. They are also increasingly used as biomarkers of oxidative stress in ecotoxicological studies[14,15].

Despite their advantages, proteomics tools face a major challenge in ecotoxicology as the lack of genomic data for many species renders the identification of particular proteins affected by treatments difficult[9]. In this context, daphnids are a prime choice as the genome of *Daphnia pulex* has recently been sequenced[16], opening the door to the application of the omics toolbox for this group of organisms. Already among the most widely-studied organisms in ecotoxicology, daphnids are routinely used to assess the toxicity of effluents and novel compounds. As the subject of many official protocols[17–19], they are an excellent model to better understand NP toxicity to the aquatic environment.

In order to better understand AgNP toxicity to aquatic organisms, this study applied a redox-proteomics approach to *D. magna*. Organisms were exposed to citrate-coated AgNP and toxicity was evaluated using a whole-organism approach and biochemical measurements. In addition to classical biomarkers, we apply for the first time the toolbox of redox-proteomics to this model organism by labelling protein carbonyls with fluorescein-5-thiosemicarbazide (FTC) prior to two-dimensional electrophoresis (2DE).

2 Results

2.1 Characterisation of AgNPs

Fig. S.1 shows a low magnification transmission electron microscope (TEM) image of the AgNPs prepared by room temperature reduction of $AgNO_3$ by $NaBH_4$ in the presence of sodium citrate as a stabiliser. The images show that the AgNPs possess a bimodal size distribution, with approximately equal numbers of both sizes. Insets to Fig. S.1 show histograms of NP diameters, determined by analysis of TEM images of 300 AgNPs of each size, all located at random locations on the grid. Fitting the histogram to a Gaussian model yielded a mean diameter for the smaller AgNPs of 3.0 ± 0.5 nm, while the larger AgNPs were more polydisperse, with a mean diameter of 11.4 ± 2.2 nm.

High-resolution TEM (HR-TEM) imaging was used in conjunction with selective area electron diffraction (SAED) to confirm the crystallinty and establish the crystal phase of the NPs; see Fig. S.2(a) and (b). HR-TEM imaging (Fig. 2(a)) showed that the AgNPs are highly crystalline; the lattice fringes shown in Fig. S.2(a) correspond to a d spacing of 2.36 Å, closely matching the (111) spacing reported for the (Fm3m) face-centred cubic lattice of silver. SAED patterns of the AgNPs (Fig. S.2(b)) showed reflections that could be indexed to 2.36 Å (111), 2.04 Å (200), 1.45 Å (220), 1.18 Å (222) and 1.02 Å (400), confirming AgNP crystallinity.

Fig. S.3 shows the energy dispersive X-ray (EDS) spectrum of the AgNPs, where the Ag peak corresponding to the presence of the NPs is evident. Other elemental peaks assigned to Cu are due to the carbon-coated copper grid support. UV-Vis absorption spectra of the freshly-prepared AgNPs exhibited a strong peak centred at 392 nm, with an absorbance (A_{392}) of 0.859 (Fig. S.4). In comparison, A_{392} for the SAgNP was less than 0.008, corresponding to a $>$ 100-fold decrease in the concentration of AgNPs following ultracentrifugation. The red-shift in the residual absorption band to 407 nm is probably due to the presence of AgNP aggregates that were temporarily re-suspended while extracting the supernatant from the centrifuge tube.

2.2 Immobilisation Assay

The impact of AgNP, silver nitrate as well as the supernatant of AgNP was measured as EC50 of immobilisation on *Daphnia magna* neonates according to established OECD[17] protocols. Results (Table 1) show a marked difference in toxicity between AgNPs (47.2 µg/L) and silver ions (4.5 µg/L). Additionally, when particles were removed from the AgNP solution by ultracentifugation, toxicity decreased by a factor of 6.3. Ageing of the particles in the stock solution in the dark did not significantly affect their toxicity.

Table 1 EC50 for the immobilisation of *Daphnia magna* by silver compounds

Compound	EC50 (µg/L)	95% CI
Fresh AgNP	47.2	43.2 – 50.5
SAgNP[a]	298.6	274.2 – 325.1
Ag^+	4.5	2.7 – 7.4
6 m.o. AgNP[b]	50.2	39.4 – 64.0
10 m.o. AgNP[b]	50.2	45.2 – 55.8
10 m.o. SAgNP[ab]	429.9	376.1 – 491.3

[a] Supernatant obtained by ultracentrifugation of the AgNP stock, toxicity is in nominal [Ag] pre-centrifugation.
[b] Toxicity of AgNP was tested after 6 and 10 months of ageing, and after 10 months for the supernatant.

2.3 Molecular Biomarkers

Enzymatic assays did not show statistically significant effects of exposure to either $AgNO_3$ or AgNP (data not shown) for concentrations of up to half their respective EC50. In comparison, relative FTC fluorescence significantly increased when *D. magna* were exposed to 20 µg AgNP/L (54% increase, $p < 0.001$) but was not affected by $AgNO_3$ exposure (Fig. 1). A trend towards an increase of IAF labelling with increasing concentrations of either AgNP or $AgNO_3$ was also observed (Fig. 1), although this increase was only statistically significant at an intermediate concentration of AgNP (15 µg AgNPs/L, 62% increase, $p < 0.01$) and at the highest [Ag^+] (2.5µg/L Ag, 63% increase, $p < 0.01$).

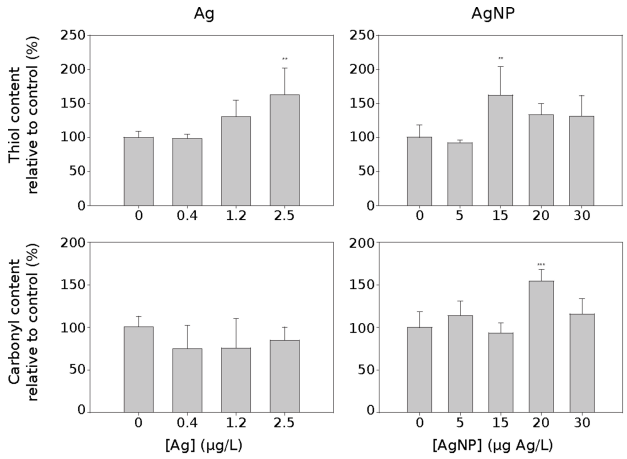

Fig. 1 Measurement of protein carbonyl and thiol content using fluorescent labels on samples exposed to silver nitrate and AgNP: Fluorescent values were normalised upon total protein stain to obtain relative fluorescence. (*: $p < 0.05$; **: $p < 0.01$; ***:$p < 0.001$)

2.4 2DE

On 2DE analysis of proteins from samples exposed to AgNP, a total of 10 unique features showed significant volume change of at least 1.5 fold, while 7 were significantly altered in silver nitrate-exposed samples, either at the protein or FTC labelling level (features are shown in Fig. 2). With increasing [AgNP], five features showed an increase of volume of protein stain, one showed decreasing protein stain volumes, two features showed increased carbonyl stain volumes and four showed decreasing carbonyl volumes. Two features (5 and 9) showed significant volume changes both for coomassie stain and FTC labelling. Under increasing [Ag^+], one feature showed an increase in protein stain volume and one a decrease, while one showed increasing carbonyl stain volumes, one a decreasing carbonyl stain volume and three showed a variable response with concentration (*e.g.*: decrease followed by an increase).

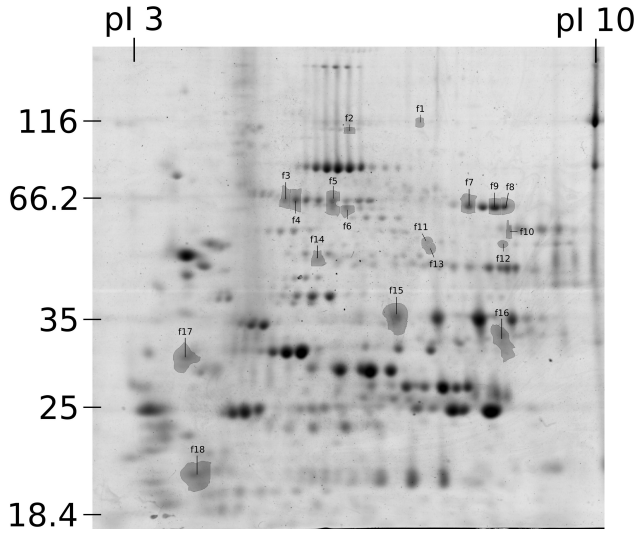

Fig. 2 2DE separation of 100 µg of *Daphnia magna* proteins showing features modified ($p < 0.05$ and > 1.5 fold change) by AgNP or $AgNO_3$ exposure

2.5 Protein identification

Of the 17 features of interest revealed by 2DE, eight were successfully identified by MS/MS analysis (Table 2). Among these, four different hypothetical proteins from the recent *Daphnia pulex* genome[16] were found. In order to gain insight into the potential function of these proteins, bioinformatics tools were used to find similar proteins and the families to which those proteins could be related. The results of these analyses are shown in Table 3. The three bioinformatic tools used (blastp, DELTA-BLAST and InterproScan) were in good agreement as to the type of protein identified here. For brevity, only the best results from the blastp search and the families and main domains found in InterproScan are included in Table 3.

Among the eight identified features, four were annotated as vitellogenin fused with superoxide dismutase (SOD), two as a vitellogenin-like protein, one as hemoglobin and one as the regulatory protein 14-3-3 epsilon. The fold change of the feature volumes from which the above proteins were identified is shown in Table 4 while the features are shown on the reference image of the analysis (Fig. 2).

3 Discussion

3.1 Whole organism toxicity

Results obtained from the immobilisation assay show a clear difference in toxicity between silver nitrate and nanoparticulate silver, with the latter appearing to be 10 times less toxic (considering Ag concentration). As many studies relate AgNP

Table 2 Identified proteins using LC-MS/MS

Feature	Protein	Organism	Accession number	MW (kDa) (Measured / Predicted)	Protein Score[a] / Protein C.I. (%)	Total Ion Score / Total Ion C.I. (%)	Sequence coverage (%)	Number of peptides[b]
f1	hypothetical protein DAPPUDRAFT_318420	*Daphnia pulex*	gi|321469729	98/171	362/100	289/100	17	3
f3	hypothetical protein DAPPUDRAFT_213992	*Daphnia pulex*	gi|321465380	68/228	153/100	153/100	10	2
f4	hypothetical protein DAPPUDRAFT_213992	*Daphnia pulex*	gi|321465380	68/228	162/100	144/100	11	2
f5	hypothetical protein DAPPUDRAFT_213992	*Daphnia pulex*	gi|321465380	68/228	205/100	162/100	16	2
f7	hemoglobin	*Daphnia magna*	gi|2105139	66/38	319/100	301/100	19	2
f10	hypothetical protein DAPPUDRAFT_313764	*Daphnia pulex*	gi|321474716	16/170	283/100	283/100	12	2
f15	vitellogenin fused with superoxide dismutase	*Daphnia magna*	gi|39979307	40/225	559/100	485/100	14	2
f18	hypothetical protein DAPPUDRAFT_326737	*Daphnia pulex*	gi|321460806	19/29	447/100	381/100	52	4

[a] The protein score probability limit (where $p < 0.05$) is 86.
[b] Number of MS/MS patterns assigned to peptides with confidence interval above 95 %.

toxicity to their slow dissolution we removed the nanoparticles from solution by ultracentrifugation to determine whether the observed toxicity was a product of dissolved silver, as shown by Kittler *et al.* [22], or if the particles were responsible for the observed toxicity. As the supernatant was 6.3 times less toxic (as measured by EC50) than the nanoparticle suspension, the observed toxicity of the AgNP is thus associated with the particles themselves and their behaviour in the medium and in contact with the organisms. The present experiment does not control for dissolution of the nanoparticles in the test medium, but the results below indicate that the nanoparticles have a different toxicity mechanism than silver nitrate.

3.2 Biomarkers

Surprisingly few effects were observed with classical biomarkers, even though exposure concentrations went as high as half the EC50 and mortality (less than 20%) was observed at the highest concentrations. Few studies have looked at the impact of AgNP or Ag^+ on daphnid enzymatic activities, but the lack of observed effects of Ag^+ may be linked to the fact that disturbances in osmoregulation are the main mechanism of toxicity of silver ions in these organisms [23]. In addition, Poynton *et al.* [8] did not find an impact of Ag^+ or AgNP on GST mRNA levels.

Although the measured enzymatic activities were not affected by the treatments, the thiol content of proteins from daphnids was increased by $AgNO_3$ and AgNP (Fig. 1). This may represent an attempt by the animals to decrease the toxicity of silver ions (which are also likely to be present in small concentrations in the AgNP exposures) as thiols are known to react with silver ions [24]. The increase of the thiol content following AgNP exposures is not expected when the usual link between AgNPs and OS is considered. Protein thiols are easily oxidised when the redox balance of the cell is disturbed, as they act both as buffers and sensors of oxidative stress in cells. The observed increase, if not linked to silver dissolved from the AgNPs, may be a result of the cell restoring its redox balance to counteract the stress of exposure. This is reinforced by the fact that there is an increase in the carbonyl content of the proteins in daphnids exposed to AgNPs but not silver nitrate (Fig. 1). Protein carbonyls are the main lesion found in proteins, as they are generated by the oxidation of various amino acids [25]. The increase in protein carbonyls indicates that some level of oxidative stress was caused by the AgNP, although not enough to also oxidise the protein thiols. In contrast, the lack of change of the level of protein carbonyls in the exposures to silver nitrate suggests that significant OS did not occur in the daphnids, perhaps as a result of the increasing thiol content with increasing silver concentration.

Table 3 Blast and interproscan search of hypothetical proteins

Feature	Accession Number	Best hit[a] (protein (*species*), E-Value, Identity %)	Families and Domains[b]	Go functions[b]
f1	gi|321469729	Vitellogenin-like protein (*Lepeophtheirus salmonis*) E: 3e-106, Identity: 24%	von Willebrand factor, type D Domain; Vitellinogen, superhelical; Vitellinogen, beta-sheet N-terminal	Lipid transport activity; Lipid transport
f3,f4,f5	gi|321465380	Vitellogenin fused with superoxide dismutase (*Daphnia magna*) E: 0.0, Identity: 52%	Superoxide dismutase (Cu/Zn)/chaperones; von Willebrand factor, type D Domain; Vitellinogen, open beta-sheet; Vitellinogen, beta-sheet N-terminal	Superoxide metabolic process; Metal ion Binding; Oxidation-reduction Process; Lipid transport activity; Lipid transport
f10	gi|321474716	Vitellogenin-like protein (*Lepeophtheirus salmonis*) E: 3e-106, Identity: 24%	von Willebrand factor, type D Domain; Vitellinogen, superhelical; Vitellinogen, beta-sheet N-terminal	Lipid transport activity; Lipid transport
f18	gi|321460806	14-3-3 protein epsilon (*Schistocerca gregaria*) E: 2e-170, Identity: 91%	14-3-3 protein	protein domain specific binding

[a] Best hit results are obtained using a blastp search [20].
[b] Families, domains and GO functions were obtained using Interproscan [21].

Table 4 Fold change of feature volumes of identified proteins[a]

	AgNP (coomassie/fluorescence)				**Ag$^+$** (coomassie/fluorescence)		
Protein (feature)	5 ppb	15 ppb	20 ppb	30 ppb	0.4 ppb	1.2 ppb	2.5 ppb
Vitellogenin-like protein (f1)	– / –	– / –	– / –	– / –	– / -1.3	– / -1.7	– / -1.1
Vitellogenin fused with superoxide dismutase (f3)	– / –	– / –	– / –	– / –	-1.1 / –	1.1 / –	1.8 / –
Vitellogenin fused with superoxide dismutase (f4)	1.1 / –	1.5 / –	1.4 / –	1.5 / –	– / –	– / –	– / –
Vitellogenin fused with superoxide dismutase (f5)	1.1 / -1.1	-1.1 / -1.4	-1.6 / -1.7	-1.4 / -1.6	– / –	– / –	– / –
Hemoglobin (f7)	1.0 / –	1.4 / –	1.3 / –	1.6 / –	– / –	– / –	– / –
Vitellogenin-like protein (f10)	– / –	– / –	– / –	– / –	– / -1.4	– / 1.0	– / 1.4
Vitellogenin fused with superoxide dismutase (f15)	– / -1.2	– / -1.5	– / -1.8	– / -1.7	– / –	– / –	– / –
14-3-3 protein epsilon (f18)	– / –	– / –	– / –	– / –	– / -1.1	– / -2.0	– / -2.0

[a] Fold changes are relative to control and given only for treatment where the feature was significantly changed (ANOVA $p < 0.05$).

3.3 Proteomics approach

The number of features evident in 2DE separations as significantly affected by both treatments was similar (10 and 7), and no feature was commonly modified by both treatments. This again suggests different toxicity pathways or mechanisms between the two forms of silver tested. When comparing the results from the protein-stained and FTC-labelled gels though, two of the modified features (f5 and f9) showed changes at the protein and carbonyl content level. This most likely means that they both contained a protein whose expression was modified, rather than carbonylation as, in both cases, the change in protein and carbonyl stain volume followed the same trend with similar fold-changes. In the case of features where a change was observed only for carbonyls or protein abundance, it is likely one was modified and not the other. More in depth analysis is required for those features in order to determine the exact level of carbonylation of the proteins concerned.

Identification of the features led to the realisation that a lot of the proteins modified showed overlap between the two compounds, as two features modified by ionic silver annotated as a vitellogenin-like protein (f1 and f10) and one as a vitellogenin fused with SOD (f3); while three features modified by AgNP contained a protein annotated as a vitellogenin fused with SOD (f4,f5 and f15). This strong overlap between the two treatments is partly a result of some features being part of the same "train" (a chain of features showing similar shape and MW, but slightly different pI). As a matter of fact, features 3, 4 and 5 were identified as the same protein and are part of the same train. It should be noted that, in the case of those features, the repetition may be due to the extensive maturation process of vitellogenins (see below).

3.4 Role of modified proteins

Mass spectrometric analysis of the significant features led to the identification of two proteins from *D. magna*: Hemoglobin (f7) and vitellogenin fused with SOD (f15). All other features that yielded results from this analysis were identified as hypothetical proteins from the recently completed *D. pulex* genome (Table 2) [16]. In order to gain insight into the role of those proteins, blastp [20], DELTA-BLAST [26] and InterproScan [21] were

used to find sequence similarity with known proteins or protein domains. In all cases, a clear result was obtained, with the three search engines yielding similar results and agreeing on the likely function of the hypothetical protein. Table 3 shows the result of this analysis. As features 3, 4 and 5 contain the same protein, three different functions were found for the hypothetical proteins. Features 1 and 10 appear to be vitellogenin-like proteins (although of different mass and pI), features 3, 4 and 5 are a vitellogenin fused with SOD and feature 18 has high sequence identity with members of the 14-3-3 protein family of regulatory proteins.

Overall, six identified features out of eight appear to be either vitellogenin-like or vitellogenin fused with SOD. At present, studies have shown the presence of two isoforms of vitellogenin fused with SOD in *D. magna*, both of which were also found here. DmagVTG1[27] was identified from feature 15, while DmagVTG2[28] was found in features 3, 4 and 5. A literature search did not enable the finding of other vitellogenins in *D. magna*, but two of the hypothetical proteins appear to be vitellogenin-like proteins. This would not be surprising considering the high rate of gene duplication found in the *D. pulex* genome[16].

In oviparous species, vitellogenins are known to be differentially regulated at the gene level under many stress circumstances, and normally undergo major PTM due to their involvement in the egg maturation process[27]. In the case of daphnids, this is also true during parthenogenetic reproduction, as the main product of DmagVTG1 is gradually cleaved during egg maturation[27]. There is no known direct association of vitellogenin expression in crustaceans to a particular stressor-type or environmental factor, in contrast to fish where it is related to oestrogenic compounds when found in males[29]. Yet work has been completed to establish vitellogenins as an easily applicable biomarker between invertebrate species, including daphnids[30]. In correspondance to this, vitellogenin has been proposed as a marker of general stress in the zebra fish, especially when egg or embryo development is followed rather than adults[31]. Unsurprisingly, all the features from which vitellogenins were identified here showed much lower masses than predicted from the whole-protein sequence. This is consistent with their function and with previous results from Kato *et al.*[27], who showed that the 220 kDa protein DmagVTG1 was gradually cleaved into different proteins of smaller size. As vitellogenin maturation is thought to be a highly regulated process affected by stressors and development stages[31,32], variations in the maturation process could be used as indicators of toxic stress. Gel-based proteomics would thus be an interesting method to study differences in cleavage-site and PTMs (*i.e.* phosphorylation, glycolysation, lipidation) of vitellogenins in daphnids.

Another point of interest concerning this protein is that vitellogenins fused with SOD were only found in daphnids[28] and in *Artemia*[32]. The presence of a SOD domain may indicate a link with oxidative stress. Hannas *et al.*[29] found that many of the stressors that upregulate DmagVTG2 are also linked to OS while Kato *et al.*[27] showed that the SOD domains present some, although weak, SOD activity. Since oxidative stress is a likely candidate for the toxicity mechanism of AgNP, this could explain the impact of those compounds on vitellogenins.

Exposure to AgNP led to an increase in hemoglobin, the main oxygen carrier in daphnids. Hemoglobin expression is known to be highly variable in daphnids, with its levels increasing when oxygen levels are low or temperatures changes rapidly[33,34], and in response to toxic stress[35]. In both cases, an increase in ROS may result in increased hemoglobin expression, as in *D. magna*, hemoglobin expression is under the control of hypoxia-inducible-factor-1 (HIF-1)[34]. The observed increase is thus a likely sign of OS, as oxygenation was maintained throughout the 24 h exposures. This also agrees with the observed increase in protein carbonylation discussed above.

Exposure to silver nitrate led to a 2-fold decrease in the level of carbonylation of a likely member of the 14-3-3 protein family. Although no studies have been published on 14-3-3 proteins in daphnids, this family of proteins is well-studied elsewhere. They have diverse roles including control of the cell cycle and apoptosis, signal transduction and regulation of the subcellular localisation of proteins. They are found in all eukaryotes[36]. In shrimps, they have been shown to be up-regulated during viral infection[37] and microbial challenge[38]. The fact that the 14-3-3 protein observed here showed a lower level of carbonylation following ionic silver exposure as well as a mass almost half that expected from the gene sequence may either indicate proteolytic cleavage of the protein (with loss of carbonylation) or a higher turnover rate, both potentially leading to changes in cell-signalling following exposure.

Globally, the response from the two forms of silver shown here is quite distinct. Although no clear conclusion can be drawn concerning the mechanism of action of AgNP, its effect seems to be quite different from that of $AgNO_3$. With the exception of features 3 and 4 (both containing DmagVTG2 and increasing in volume with exposure concentration), all features were modified by only one of the two forms of silver tested. In addition to the fact that toxicity of the AgNP preparation was strongly reduced following centrifugation, we propose that the particles present a toxicity different from that of silver ions, albeit at a lower level. This is in contradiction to previous studies and the general understanding that a major portion of AgNP toxicity originates from their dissolution[22]. Yet this is in agreement with other studies in daphnids where particles were found to be less toxic than silver nitrate[7] and where particle toxicity did not follow the same mechanism as silver nitrate toxicity[8]. Although our results do not give clear

insight into the mechanism of toxicity of AgNP, the difference observed between the effects of AgNP and Ag^+ at the molecular level indicate that the two species of silver affect daphnids differently. Whether this is an effect of whole particles acting directly at the cellular level as is known for metal NPs of similar sizes or from the particles acting as "delivery" vehicles for ionic silver to specific parts of the daphnid cannot be concluded from the present study.

4 Experimental

4.1 Chemicals

The Protein Assay Dye Reagent concentrate was obtained from Bio-Rad (CA, USA). Unstained protein molecular weight markers for SDS-PAGE were from Thermo Scientific (Rockford, IL, USA). Immobiline Drystrips and IPG buffer were obtained from GE Healthcare (UK). All other chemicals were sourced from Sigma-Aldrich Ireland Ltd. (Arklow, Co. Wicklow) and used as received.

4.2 Synthesis and characterisation of AgNPs

Nanopure H_2O (18.2 MΩ cm), purified using an Elgastat Prima purification system, was employed during all experiments. All synthetic glassware was first cleaned with Aqua Regia (3 HCl: 1 HNO_3), and then thoroughly rinsed with deionised water. In a typical synthesis, 12 mL of a 0.2% solution of silver nitrate was added to 488 mL of deionized water and heated to 100 °C. 11.6 mL of a 1% solution of sodium citrate in deionised water was added, followed 30 s later by the quick injection of 5.5 mL of a freshly prepared, ice-cold solution of 0.038 g sodium borohydride and 0.5 g sodium citrate in 50 mL deionised water. The solution was stirred for two minutes, after which it was cooled to room temperature, and stored in the dark.

UV-Vis absorption spectra were recorded using a Shimadzu UV PC-2401 spectrophotometer equipped with a 60 mm integrating sphere (ISR-240A, Shimadzu). Spectra were recorded at room temperature using a quartz cuvette (1 cm) and corrected for the solvent absorption. AgNP and SAgNP samples were diluted 1:5 in deionised water for spectroscopic comparison. TEM images and SAED patterns were acquired using a high-resolution JEOL 2100 electron microscope, equipped with a LaB_6 thermionic emission filament and Gatan DualVision 600 Charge-Coupled Device (CCD), operating at an accelerating voltage of 200 keV. EDS were recorded using an Oxford INCA x-sight detection spectrometer. Spectra were obtained from an area of the grid where there was a large amount of NPs. A process time of 3-4 seconds was used and the spectra obtained using an integration time of 40 s. TEM samples were prepared by depositing a small aliquot of the AgNPs onto a carbon-coated copper grid (Agar Scientific), which was allowed to evaporate under ambient conditions. Data for size distribution histograms were acquired by analysis of TEM images of NPs randomly located at different regions of the grid. NP diameter was determined by manual inspection of the digital images; in the case of anisotropic structures, the diameter was determined using the longest axis.

4.3 AgNP supernatant

To remove particles from solution, the AgNP solution was centrifuged at 100 000 g for 30 min. Supernatants were then used in the same way as the particle suspension. In order to better illustrate the impact of particle removal on toxicity, supernatant "concentration" is noted in [Ag] equivalents: the nominal concentration of Ag the solution would contain if particles had not been removed. Before use, supernatants were kept in the dark at room temperature.

4.4 *Daphnia magna* culture

A clonal culture of *D. magna* was maintained in Elendt M4 medium[39] in plastic aquaria at 20 ± 1 °C with a 16:8 light-dark cycle and constant bubbling. *D. magna* were fed live *Chlorella vulgaris* to a concentration of 50 000 cells per mL at least 4 times per week. Brood stocks were maintained at 50 females per 4 L. Half the medium was renewed two or three times per week. Neonates were removed at least three times per week. Prior to exposures, neonates were kept for 7 days (in 10 mL of medium per neonate), with daily feed of *C. vulgaris*, in order to obtain enough tissue for biochemical assays.

4.5 Immobilisation assay

All assays were performed according to OECD[17] recommendations. At least 30 neonates were exposed, in 4 mL M4 per neonate, in glass beakers at 20 ± 1 °C under a 16:8 light-dark cycle. Immobilisation was observed after 24 and 48 hours. Results were fitted with a two-parameter log-logistic model using the dcr package in R[40,41] in order to estimate EC50 values. Unless stated otherwise, assay to AgNP and their supernatants were conducted within a week of AgNP synthesis.

4.6 Exposures

All exposures for biochemical measurements were performed for 24 h using 7 days old *D. magna* in 1 L glass beakers at 100 daphnids per beaker in the same conditions as culture. Daphnids were exposed to four concentrations of AgNP (5, 15, 20 and 30 µg Ag/L) and three concentrations of $AgNO_3$ (0.4; 1.2 and 2.5 µg Ag/L). All exposures were repeated four times and control exposures were ran in parallel. Exposures to AgNP were conducted within a week of synthesis. At the

end of the exposure, live daphnids were sieved and blotted dry before transfer to a microcentrifuge tube and flash freezing in liquid N_2, they were then kept at -80 °C until homogenisation.

4.7 Homogenisation and enzymatic assays

Nitrogen bubbled homogenisation buffer (10 mM tris HCl, pH 7.2, 0.5 M sucrose, 0.15 M KCl, 1 mM EDTA and 1 mM PMSF) was added to frozen daphnids (300 µL for one hundred 7 days old daphnids) in a glass-teflon homogeniser, prior to motor-driven homogenisation for one minute. Homogenates were then centrifuged at 14 000 g for 1 h, pellets were discarded and supernatants were aliquoted for biochemical assays. These were either performed on the day of homogenisation or aliquots were frozen at -80 °C immediately.

Protein concentrations were assessed by a Bradford assay[42] in microtiter plates as per manufacturer's instructions (Bio-Rad Protein Assay Dye Reagent).

Catalase assays were performed according to the method of Beers and Sizer[43]. Briefly, 5 µg protein was added to 16.7 mM phosphate buffer, pH 7.0, containing 19.7 mM hydrogen peroxide. A_{240} was measured immediately for 3 minutes using a dual-beam spectrophotometer and a quartz cuvette. One unit of activity was defined as the decomposition of one micromole of peroxide per minute in the assay conditions used. Glutathione transferase activity was assessed using the conjugation of 1-chloro-2,4-dinitrobenzene (CDNB) with reduced glutathione, according to Habig *et al.*[44] using a protocol modified for microtiter plates. Briefly, 8 µg protein was added to a final reaction mixture of 75 mM phosphate buffer, pH 6.5, 1 mM CDNB and 5 mM reduced glutathione (added last to initiate the reaction). Activity was followed by the increase of A_{340} and one unit is defined as the production of one micromole of conjugate per minute. Glyceraldehyde-3-phosphate dehydrogenase (GAPDH) activity was measured in microtiter plates by following the reduction of NAD in the presence of glyceraldehyde-3-phosphate[45]. Five µg protein was added to a reaction mixture containing 15 mM sodium pyrophosphate buffer, pH 8.5, 30 mM sodium arsenate, 0.25 mM NAD, 3.25 mM dithiothreitol and 12.5 mM DL-glyceraldehyde-3-phosphate (added last to initiate the reaction). Activity was followed as an increase in A_{340} and one unit is defined as the reduction of one micromole of NAD per minute.

4.8 PTM labelling and one-dimensional electrophoresis

In order to estimate protein thiol content, 100 µg protein was labelled with 5-(iodoacetamido)fluorescein (IAF). IAF was added to homogenates from a 20 mM stock in DMSO to a final concentration of 0.2 mM, and incubated at 4 °C for 2 h in the dark[46]. Proteins were then precipitated by adding trichloroacetic acid (TCA) to a final concentration of 10% w/v, incubated on ice for 5 min and centrifuged at 11 000 g for 3 min. The pellet was resuspended in 40 µL of water, and 500 µL of acetone was added to remove unbound IAF. Samples were then kept at -20 °C for at least one hour. Before electrophoresis, proteins were centrifuged at 11 000 g for 3 min, acetone was removed, and pellets were dried in the dark. Sample buffer was added to solubilise the proteins and those were run on 10% polyacrylamide gels, at a loading of 20 µg per lane, with four replicate lanes per sample, as per Laemmli[47]. After electrophoresis, gels were scanned using a Typhoon scanner, model 9410 (Amersham Biosciences), with an excitation wavelength of 488 nm and emission light of 520 ± 20 nm (bandpass filter). After acquisition of the fluorescence image, gels were stained with colloidal coomassie[48], and gel images were acquired with a GS-800 Calibrated Densitometer (BioRad, Hercules, CA, USA).

Protein carbonyls were labelled by adding (FTC) to tissue homogenates (100 µg) to a final concentration of 1 mM (adapted from Chaudhuri *et al.*[49]). Samples were incubated for 2h in the dark at 4 °C before precipitation of proteins with a final concentration of 10% w/v of TCA. Pellets were washed twice with 500 µL of ice cold 1:1 ethanol:ethylacetate. Prior to resuspension and electrophoresis as above, pellets were centrifuged and dried to make sure no solvent remained in the samples. Gels containing FTC labelled samples were scanned for fluorescence and protein content as described above.

4.9 Two-dimensional electrophoresis and protein identification

Aliquots of freshly prepared homogenates containing 500 µg protein were labelled with FTC as above, with the exception that rehydration buffer (5 M urea, 2 M thiourea, 2% w/v CHAPS, 2% IPG buffer) was used to resuspend the pellets. Of this, 125 µL, containing 125 µgprotein, were loaded unto an Immobiline DryStrip (pH 3-10 NL, 7 cm, GE Healthcare), which was rehydrated overnight in the dark. Isoelectric focusing was performed on a PROTEAN IEF system (Bio-Rad), according to the strip manufacturer's recommendation. Strips were reduced in equilibration buffer (6 M urea, 0.375 M Tris, pH 8.8, 2% w/v SDS, 20% v/v glycerol) containing 2% w/v DTT for 20 min and thiols were then blocked with equilibration buffer containing 2.5% w/v iodoacetamide for 20 min. After focusing, strips were loaded unto 10% polyacrylamide gels for SDS-PAGE separation. Gels were scanned for fluorescence and then stained with colloidal coomassie as for 1DE. Image analysis was performed using the Progenesis SameSpots software (Nonlinear Dynamics Limited, UK). Experiments were defined by compound, with the exposure concentrations representing treatments. Spots were considered of interest when showing a 1.5 fold change between treatments as well as having a $p < 0.05$ in ANOVA. Significant, well re-

solved spots of sufficient intensity were then selected for mass spectrometric analysis.

Selected spots were excised manually using clean pipette tips and in-gel digested with trypsin according to Almeida *et al.* [50]. Extracted peptides were loaded onto a R2 micro column (RP-C18 equivalent) where they were desalted, concentrated and eluted directly onto a MALDI plate using α-ciano-4-hydroxycinamic acid as the matrix solution in 50% acetonitrile and 5% formic acid. Mass spectra of the peptides were acquired with positive reflectron MS and MS/MS modes using a MALDI-TOF/TOF MS instrument (4800 plus MALDI TOF/TOF analyzer) with exclusion list of the trypsin autolysis peaks (842.51, 1045.56, 2211.11 and 2225.12). The collected MS and MS/MS spectra were analysed in combined mode by using the Mascot search engine (version 2.2; Matrix Science, Boston, MA) and the NCBI database restricted to 50 ppm peptide mass tolerance for the parent ions, an error of 0.3 Da for the fragments, one missed cleavage in peptide masses, and carbamidomethylation of Cys and oxidation of Met as fixed and variable amino acid modifications, respectively. No taxonomy restrictions were applied. The identified proteins were only considered if a MASCOT score above 95% confidence was obtained ($p < 0.05$) and at least one peptide was identified with a score above 95% confidence ($p < 0.05$). This analysis was conducted by the Analytical Services Unit, Instituto de Tecnologia Qumica e Biolgica (ITQB), New University of Lisbon, Lisbon, Portugal.

4.10 Data analysis

Images from 1DE were analysed with the Quantity One software (Bio-Rad) to obtain one trace measurement per lane. Fluorescence values were normalised for loading by dividing them with the trace coomassie value for the same lane. Statistical analysis of enzymatic and PTM assays were performed by one-way ANOVA with a Holm-Sidak post-hoc test (versus control), using the Sigmaplot 10.0 software (Systat Software, Inc.).

4.11 Hypothetical proteins

Hypothetical proteins (HP) identified by MS/MS were studied using bionformatics tools to gain insight into their possible biological functions. This was achieved using blastp [20] and DELTA-BLAST [26] from the National Center for Biotechnology Information (`http://blast.ncbi.nlm.nih.gov/Blast.cgi`) to identify sequence similarity with known proteins. In addition, conserved sites, domains and families present in the HP were studied using the Interproscan tool [21] from the European Bioinformatics Institute (`http://www.ebi.ac.uk/Tools/pfa/iprscan/`). Results include the highest-scoring, non-hypothetical, protein from blastp, as well as the domains and families identified from Interproscan. In the present study, those were always in accordance with results from DELTA-BLAST

5 Conclusions

This study compared the toxicity of citrate-coated AgNP and silver nitrate to *D. magna* at the organism level, using biochemical biomarkers and with redox-proteomic tools. AgNP were found to be about ten times less toxic than silver nitrate. Although measured enzymatic activities (GST, catalase and GAPDH) were not affected by the treatments, an increase of protein carbonylation was observed following AgNP exposure, indicating OS, while no sign of OS was found for $AgNO_3$ exposure. Proteins identified following 2DE separation showed signs of general stress, with most of the features modified by the treatments containing vitellogenins, indicating that the maturation process or expression of vitellogenins is affected, in different ways, by silver nitrate as well as AgNP. Hemoglobin was also increased by AgNP treatment, which may be linked to disruption of cellular respiration.

Overall, different molecular responses were found for the two forms of silver. Although more studies are required to better understand AgNP toxicity, the lower toxicity of AgNP often reported relative to silver ions [6,7] does not warrant its relative innocuity, as different toxicity mechanisms may mean different toxic interactions or lead to population effects that cannot be predicted by the relative EC50 of the two forms of silver.

6 Acknowledgements

This work was supported by the Irish Higher Education Authority under the PRTLI program (cycle 3 Nanoscience and Cycle 4 INSPIRE). Louis-Charles Rainville was funded by the Irish Research Council for Science, Engineering and Technologie and by the Fond Qubcois de la Recherche sur la Nature et les Technologies.

References

1 I. Bhatt and B. N. Tripathi, *Chemosphere*, 2011, **82**, 308–317.
2 A. Elsaesser and C. V. Howard, *Adv. Drug Delivery Rev.*, 2012, **64**, 129–137.
3 S. J. Klaine, P. J. J. Alvarez, G. E. Batley, T. F. Fernandes, R. D. Handy, D. Y. Lyon, S. Mahendra, M. J. McLaughlin and J. R. Lead, *Environ. Toxicol. Chem.*, 2008, **27**, 1825–1851.
4 Z. Yuan, Y. Chen, T. Li and C.-P. Yu, *Chemosphere*, 2013, **93**, 619–625.
5 R. Kaegi, A. Voegelin, B. Sinnet, S. Zuleeg, H. Hagendorfer, M. Burkhardt and H. Siegrist, *Environ. Sci. Technol.*, 2011, **45**, 3902–3908.
6 B. M. Angel, G. E. Batley, C. V. Jarolimek and N. J. Rogers, *Chemosphere*, 2013, **93**, 359–365.

7 I. Blinova, J. Niskanen, P. Kajankari, L. Kanarbik, A. Käkinen, H. Tenhu, O.-P. Penttinen and A. Kahru, *Environ. Sci. Pollut. Res.*, 2013, **20**, 3456–3463.

8 H. C. Poynton, J. M. Lazorchak, C. A. Impellitteri, B. J. Blalock, K. Rogers, H. J. Allen, A. Loguinov, J. L. Heckman and S. Govindasmawy, *Environ. Sci. Technol.*, 2012, **46**, 6288–6296.

9 T. Monsinjon and T. Knigge, *Proteomics*, 2007, **7**, 2997–3009.

10 D. Sheehan, B. McDonagh and J. A. Bárcena, *Expert Rev. Proteomics*, 2010, **7**, 1–4.

11 M. Bruschi, G. Candiano, L. D. Ciana, A. Petretto, L. Santucci, M. Prunotto, R. Camilla, R. Coppo and G. M. Ghiggeri, *J. Chromatogr., B: Anal. Technol. Biomed. Life Sci.*, 2011, **879**, 1338–1344.

12 E. R. Stadtman, *Free Radical Res.*, 2006, **40**, 1250–1258.

13 C. M. Wong, L. Marcocci, L. Liu and Y. J. Suzuki, *Antioxid. Redox Signaling*, 2010, **12**, 393–404.

14 B. C. Almroth, J. Sturve, E. Stephensen, T. F. Holth and L. Förlin, *Mar. Environ. Res.*, 2008, **66**, 271–277.

15 B. Ching, S. F. Chew, W. P. Wong and Y. K. Ip, *Aquat. Toxicol.*, 2009, **95**, 203–212.

16 J. K. Colbourne, M. E. Pfrender, D. Gilbert, W. K. Thomas, A. Tucker, T. H. Oakley, S. Tokishita, A. Aerts, G. J. Arnold, M. K. Basu *et al.*, *Science*, 2011, **331**, 555–561.

17 OECD, *Daphnia sp., Acute Immobilisation Test*, Organisation for Economic Cooperation and Development, 2004.

18 EC, *Biological test method: test of reproduction and survival using the cladoceran Cerodaphnia dubia*, Environment Canada, 2nd edn, 2007.

19 USEPA, *Short-term methods for estimating the chronic toxicity of effluents and receiving waters to freshwater organisms*, United States Environmental Protection Agency, 4th edn, 2002.

20 S. F. Altschul, T. L. Madden, A. A. Schäffer, J. Zhang, Z. Zhang, W. Miller and D. J. Lipman, *Nucleic Acids Res.*, 1997, **25**, 3389–3402.

21 E. Quevillon, V. Silventoinen, S. Pillai, N. Harte, N. Mulder, R. Apweiler and R. Lopez, *Nucleic Acids Res.*, 2005, **33**, W116–W120.

22 S. Kittler, C. Greulich, J. Diendorf, M. Köller and M. Epple, *Chem. Mater.*, 2010, **22**, 4548–4554.

23 A. Bianchini and C. M. Wood, *Environ. Toxicol. Chem.*, 2003, **22**, 1361–1367.

24 S. W. Wijnhoven, W. J. Peijnenburg, C. A. Herberts, W. I. Hagens, A. G. Oomen, E. H. Heugens, B. Roszek, J. Bisschops, I. Goesens, D. van de Meent, S. Dekkers, W. H. de Jong, M. van Zijverden, A. J. Sips and R. E. Geertsma, *Nanotoxicology*, 2009, **3**, 109–138.

25 E. R. Stadtman and R. Levine, *Ann. N.Y. Acad. Sci.*, 2000, **899**, 191–208.

26 G. M. Boratyn, A. A. Schaffer, R. Agarwala, S. F. Altschul, D. J. Lipman and T. L. Madden, *Biol. Direct*, 2012, **7**, 12.

27 Y. Kato, S. ichi Tokishita, T. Ohta and H. Yamagata, *Gene*, 2004, **334**, 157–165.

28 S.-i. Tokishita, Y. Kato, T. Kobayashi, S. Nakamura, T. Ohta and H. Yamagata, *Biochem. Biophys. Res. Commun.*, 2006, **345**, 362–370.

29 B. R. Hannas, Y. H. Wang, S. Thomson, G. Kwon, H. Li and G. A. Leblanc, *Aquat. Toxicol.*, 2011, **101**, 351–357.

30 G. Jubeaux, F. Audouard-Combe, R. Simon, R. Tutundjian, A. Salvador, O. Geffard and A. Chaumot, *Environ. Sci. Technol.*, 2012, **46**, 6315–6323.

31 U. Gündel, D. Benndorf, M. von Bergen, R. Altenburger and E. Küster, *Proteomics*, 2007, **7**, 4541–4554.

32 S. Chen, D.-F. Chen, F. Yang, H. Nagasawa and W.-J. Yang, *Biol. Reprod.*, 2011, **85**, 31–41.

33 P. J. Williams, K. B. Dick and L. Y. Yampolsky, *Evol. Ecol.*, 2012, **26**, 591–609.

34 D. Becker, B. F. Brinkmann, B. Zeis and R. J. Paul, *Biol. Cell*, 2011, **103**, 351–363.

35 B. T. A. Muyssen, M. Messiaen and C. R. Janssen, *Ecotoxicol. Environ. Saf.*, 2010, **73**, 735–742.

36 M. J. van Hemert, H. Y. Steensma and G. P. H. van Heusden, *BioEssays*, 2001, **23**, 936–946.

37 P.-o. Chongsatja, A. Bourchookarn, C. F. Lo, V. Thongboonkerd and C. Krittanai, *Proteomics*, 2007, **7**, 3592–3601.

38 N. He, H. Liu and X. Xu, *Fish Shellfish Immunol.*, 2004, **17**, 121–128.

39 B.-P. Elendt and W. Bias, *Water Res.*, 1990, **24**, 1157–1167.

40 R Core Team, *R: A language and Environment for Statistical Computing*, R Foundation for Statistical Computing, Vienna, Austria, 2013.

41 C. Ritz and J. C. Streibig, *J. Stat. Softw.*, 2005, **12**, 1–22.

42 M. M. Bradford, *Anal. Biochem.*, 1976, **72**, 248–454.

43 R. F. Beers, Jr. and I. W. Sizer, *J. Biol. Chem.*, 1952, **195**, 133–140.

44 W. H. Habig, M. J. Pabst and W. B. Jakoby, *J. Biol. Chem.*, 1974, **249**, 7130–7139.

45 E. Krebs, *Methods in Enzymology*, Academic Press, 1955, vol. 1.

46 J. W. Baty, M. B. Hampton and C. C. Winterbourn, *Proteomics*, 2002, **2**, 1261–1266.

47 U. K. Laemmli, *Nature*, 1970, **227**, 680–685.

48 N. Dyballa and S. Metzger, *Fast and sensitive colloidal coomassie G-250 staining for proteins in polyacrylamide gels*, 2009, `http://www.jove.com/index/Details.stp?ID=1431`.

49 A. R. Chaudhuri, E. M. de Waal, A. Pierce, H. V. Remmen, W. F. Ward and A. Richardson, *Mech. Ageing Dev.*, 2006, **127**, 849–861.

50 A. M. Almeida, A. Campos, R. Francisco, S. van Harten, L. A. Cardoso and A. V. Coelho, *Anim. Genet.*, 2010, **41**, 260–272.